J. Braz. Chem. Soc., Vol. 13, No. 2, 270-275, 2002.
Printed in Brazil - ©2002 Sociedade Brasileira de Química
0103 - 5053 $6.00+0.00

Article

Structural and Morphological Characterization of the PP-0559 Kaolinite from the Brazilian Amazon Region

***Kátia C. Lombardi*[a], *José L. Guimarães*[a], *Antonio S. Mangrich*[a], *Ney Mattoso*[b], *Miguel Abbate*[b], *Wido H. Schreiner*[b] *and Fernando Wypych*[*a]**

[a] *Departamento de Química, Universidade Federal do Paraná, CP 19081, 81531-990, Curitiba – PR, Brazil*

[b] *Departamento de Física, Universidade Federal do Paraná, CP 19081, 81531-990, Curitiba – PR, Brazil*

Caulinita natural proveniente da região amazônica (PP-0559) foi caracterizada morfologica e estruturalmente com o objetivo de contribuir para o entendimento do papel da caulinita em reações redox no meio ambiente. Através de microscopia eletrônica de transmissão e difração de elétrons, confirmou-se a estrutura triclínica em cristais orientados, com diâmetros entre 0,2 e 2 μm e cerca de 50 nm de espessura. Os cristais anisotrópicos após orientação foram estudados por ressonância paramagnética eletrônica em função da direção do campo magnético aplicado. Foram estudadas as principais linhas da impureza de Fe^{+3} substitucional e centros paramagnéticos induzidos por radiação, possíveis centros oxidantes da caulinita.

We report a structural and morphological characterization of the natural kaolinite PP-0559, from the Brazilian Amazon region, with the aim to contribute to the understanding of this clay mineral in environmental redox reactions. The triclinic structure was confirmed by transmission electron microscopy and electron diffraction studies. It exhibits oriented crystals, with diameters between 0.2 and 2 μm and about 50 nm of thickness. The anisotropic crystals after orientation were studied by electron paramagnetic resonance as a function of the applied magnetic field. The main EPR absorption lines of the substitutional Fe^{+3} impurity and radiation induced paramagnetic centers were studied as possible oxidizing centers of kaolinite.

Keywords: kaolinite, clay minerals, EPR spectroscopy

Introduction

Clay minerals are the main colloidal soil fraction. Their physico-chemical properties are fundamentally influenced by their composition and surface reactivity. They present acidic catalytic and redox properties that promote the polymerization of organic residual substrates which strongly contribute to their humification.[1] The mechanisms promoting organo-mineral complex formation are very important also in the maintenance of a micronutrient reservoir for crops. These clay mineral systems are therefore important for agricultural activities in tropical countries.[2]

Stable defects in the kaolinite structure, which are detectable through electron paramagnetic resonance spectroscopy (EPR), have been associated with their habilities to polymerize amines and amino acids.[3] Thus, the comprehension of the structural and surface properties of clay minerals is fundamentally important to various scientific enterprises, such as soil and environmental sciences, as well as special advanced materials.

Kaolinite, $Al_2Si_2O_5(OH)_4$ is a dioctahedral layered hydrated aluminosilicate of the 1:1 type with two distinct interlayer surfaces. One side of the layer is gibbsite-like with aluminum atoms coordinated octahedrically to corner oxygen atoms and hydroxyl groups. The other side of the layer is constituted by a silica-like structure, where the silicon atoms are coordinated tetrahedrically to oxygen atoms (Figure 1). The adjacent layers are linked by hydrogen bonding involving aluminol (Al-OH) and siloxane (Si-O) groups. These bonding forces hinder the intercalation processes, but the hydroxyl groups on the aluminum side of the layer are passive to solvation and covalent grafting reactions.

Depending on its natural genesis, kaolinite displays low, medium or high crystal order, which determines the chemical reactivity of the clay. Isomorphic substitution of the Al^{3+} atoms by Fe^{2+} and Fe^{3+} is very common. Fe^{3+} is one

* e-mail: wypych@quimica.ufpr.br

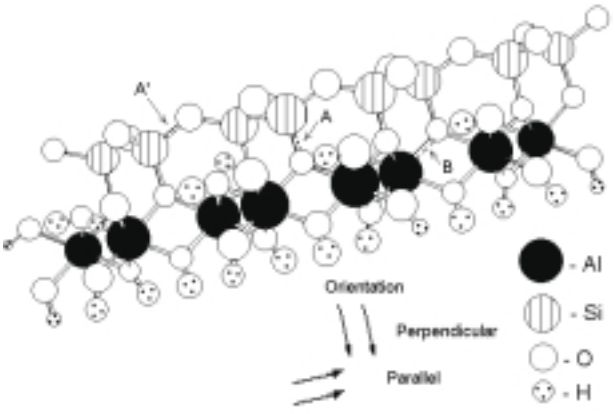

Figure 1. Detailed scheme of the kaolinite structure, with localized A, A' and B paramagnetic centers. (Reworking of an original figure with kind permission of the Virtual Museum of Minerals and Molecules™, 2000[19])

of the most common impurities in the kaolinite structure and is detected by EPR. A low cation exchange capability is generally attributed to this mineral.

Information from spectroscopic methods has resulted in a better understanding of some of the geochemical processes that control the surface and bulk composition of these minerals.[4]

Ionizing energetic particles resulting from nuclear decay in soils can drag out electrons from Si-O bonds originating the so called A and A' paramagnetic centers, while the removal of one electron from the Al-O bonding, produces the B paramagnetic centers. Figure 1 shows a schematic kaolinite structure in perspective with the assigned A, A' and B paramagnetic centers.

EPR studies have shown that iron present in the materials issued from enriched kaolinites is partly at the surface, located on the grains' outer surfaces, and partly structural, in substitutional octahedral sites.[5] The substitutional iron can be used as a sensitive probe for the degree of disorder of natural kaolinites.[6,7]

A new appraisal of radiation-induced defects in oriented natural kaolinite was undertaken using Q-band EPR spectra,[8] in which the three different centers were better identified. The trapped holes on oxygen from Si-O, A and A' centers, have a distinct signature and orthogonal orientation, perpendicular and parallel to the plane sheet, respectively. The B center is a hole trapped on the oxygen bonding Al in adjacent octahedral positions [Al(octahedral)-O-Al(octahedral)].

The A center, stable at the geological scale, was thought to have particular relevance to quantify past transits of radionuclides in the geosphere.[9] The stability of A centers seems to decrease with the increasing crystalline disorder and is high enough for radiation dosimetry using kaolinites from any environment on the Earth's surface.[8]

The present characterization of the natural kaolinite from the Brazilian Amazon region was carried out by powder X ray diffraction, transmission electron microscopy (TEM) and X ray photoelectron spectroscopy (XPS) analysis. No attempt to compare this kaolinite with samples from other places, not even from Brazil was undertaken. A detailed electron paramagnetic resonance spectroscopy (EPR) study on oriented samples was performed.

Experimental

The kaolinite sample used in this work (PP-0559) was supplied by the Petrobras Research Center (CENPES- Rio de Janeiro). It was received as a finely divided white-yellowish powder of great purity and high crystal order, mined in the Brazilian State of Pará in the Amazon Basin and was used without further purification. The high purity of the samples was confirmed by X ray fluorescence study as described previously.[10]

For the powder X ray diffraction analysis, the solid material was placed as an oriented film on a planar glass sample holder. It was oriented by suspending the kaolinite powder in water, dripping the suspension on the sample holder and drying naturally in air. The measurements were done on a Rigaku diffractometer in the Bragg-Brentano geometry using Ni-filtered CoK_{α} radiation (λ = 1.790 Å) with a dwell time of 1°/min. All measurements were taken using a generator voltage of 40 kV and an emission current of 20 mA. To remove undesirable background radiation between sample and detector a graphite monochromator was used.

The morphological and electron diffraction study was performed in a JEOL 1200 EX-II transmission electron microscope operating at 60 kV. The kaolinite crystals were suspended in water with manual stirring, deposited by casting directly on the copper grid (diameter of 3 mm) previously covered with parlodium film and dried at room temperature for several hours. Size distribution experiments confirmed that 97% of the crystals have diameter smaller than 2 μm.

The XPS spectra were taken using a VG ESCA 3000 system with a base pressure of $2x10^{-10}$ mbar. No attempt to remove the surface contaminants was undertaken. The spectra were collected using MgK_{α} radiation and the overall energy resolution was approximately of 0.8 eV. The energy scale was calibrated using the Fermi level and the adventitious C 1s peak at 284.5 eV. The spectra were normalized to the maximum intensity after a constant background subtraction.

For the EPR studies, the kaolinite sample as a powder was suspended trough mechanical stirring in distilled and deionized water and centrifuged. The wet sample, which presented a mud texture, was dropped into the plane cavity of an EPR quartz biological tissue cell and left to dry in air. For the EPR spectrum registration, the plane of the cell cavity was oriented parallel or perpendicular relative to the magnetic field of the spectrometer. EPR spectra were obtained at 298 K on a Bruker ESP 300E equipment, using a modulation frequency of 100 kHz operating at 9.5 GHz (X-band) with power of 2 mW and modulation amplitude of 5 G. All the spectra were normalized for adequate comparison.

Results and Discussions

X ray diffraction

The X ray diffractogram of the PP-0559 oriented kaolinite is illustrated in Figure 2. Only the basal plane diffraction peaks are visible. This evidences that kaolinite platelets are oriented parallel to the glass sample holder surface. Kaolinite has a triclinic structure, where the *a* and *b* crystal unit cell vectors are in plane with the kaolinite sheets, while the *c* lattice parameter vector is not collinear to the sheet normal. The high quality of the PP-0559 sample is comparable to results reported on the literature.[11] The d(001) interplanar distance is in accordance with the literature.[12] We emphasize that this diffraction result is not meant to characterize this particular kaolinite completely, as has been done many times before, but to show that this mineral is perfectly orientable on a plane sample holder.

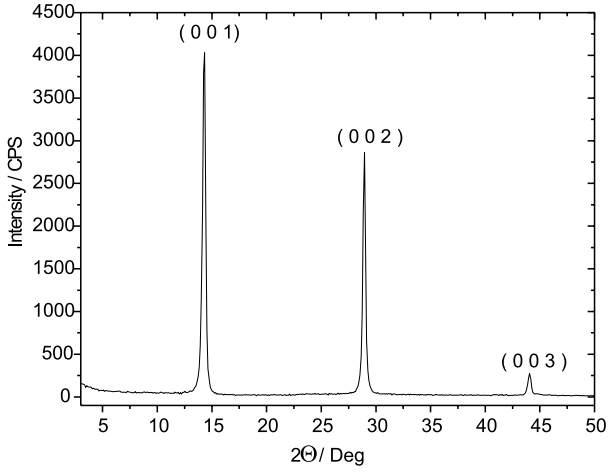

Figure 2. X-ray powder diffractogram of a PP-0559 oriented kaolinite film

Morphological Analysis

The kaolinite morphology is illustrated in Figure 3, where transmission electron micrographs with magnifications of 15000x (a) and 150000x (b) were taken. The sample is composed of highly perfect thin platelets of 0.2 to 2 μm, showing a morphology with slightly distorted hexagonal edges and corner angles of approximately 120°. Figure 3 reveals that the platelets have a tilted border. This tilted border is obviously, the macroscopic evidence of the triclinic unit cell. By measuring the width of this border on the micrograph and using the inclination of the crystal "c" axis relative to the plane separation[12] leads us to estimate the thickness of the platelets at about 50 nm.

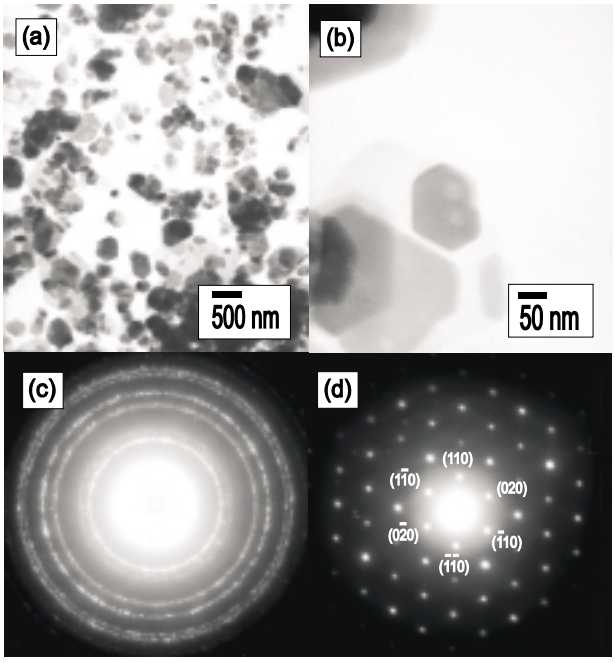

Figure 3. Transmission electron micrographs of PP-0559 kaolinite with magnifications of 15000 x (a) and 150000 x (b). Selected area electron diffraction results are shown in (c) for several kaolinite platelets and in (d) for a single platelet revealing the single crystal nature

Electron diffraction results

Figure 3 (c) shows the selected area electron diffraction pattern corresponding to an area with a 300 mm diameter, thus including multiple kaolinite platelets. The diffraction rings can be indexed as related to (020), and (1$\bar{1}$0) planes, for the first ring (the most internal); to the and (1$\bar{3}$0) planes for the second ring and to the (040) plane for the third ring. This observation is an evidence that all the crystals contain the c-axis almost parallel to the electrons beam, indicating the same texture observed in the X ray diffractogram shown in Figure 2.

Figure 3 (d) shows a diffraction pattern of a single 2 μm platelet. This pattern is obviously that of a single crystal, where the slightly distorted hexagon appears again clearly, showing the spots to which we assign the (0 2 0) and (1 1 0) indexed crystal planes. The interplanar distance values of the assigned planes are indeed the correct kaolinite values.[12]

X ray photoelectron spectroscopy

Figure 4 shows a wide scan XPS spectrum of the kaolinite sample. The C1s peak, which is due to adventitious carbon on the sample, was used as the binding energy reference (284.5 eV) for the spectrum.[13] This is necessary due to sample charging effects during the XPS measurements. Considering that this sample is commercial, the remarkable aspect is the purity, since only the Al, Si and O signatures are present in the spectrum.[14] This remarkable purity can be compared to *e.g.* Kim *et al.*,[15] which show Zn, Na and Ca in measurable quantities in kaolinite and Barr *et al.*,[16] which described a kaolinite sample with Mg, Ca and Na impurities. Otherwise, the Al, Si and O peak binding energies of the PP-0559 sample are in agreement with the results described by Kim *et al*. and Barr *et al*. Figure 5 shows the valence band XPS spectrum. The Fermi level is clearly in the band gap. The broad peak features are due to Al, Si 3p and 3s and O 2p bonding molecular orbitals while the higher peak at the right of the spectrum is due to O 2s orbitals. The general features of the valence band spectrum are in good general agreement with the results reported by Barr *et al*.,[16] reflecting the separate tetrahedral and octahedral layers contributions.

Electron paramagnetic resonance

Figure 6 shows the first derivative mode EPR spectra at a magnetic field range of 5000 G with the sample oriented relatively to the magnetic field of the spectrometer. In one of the spectra ($\perp$), the magnetic field is perpendicular to the sample face and therefore near to the perpendicularity of the kaolinite layers.

In the other spectrum ($\parallel$), the field is preferentially directed parallel to the layers. In the kaolinite sheet plane the crystal orientation is still random. There are five main lines in the spectra at magnetic fields below 2500 G, which are characteristic of low defect kaolinites with g-values of 9.0, 5.0, 4.3, 3.5 and 2.8. Those lines are due to absorptions of Fe^{3+} in both $Fe_{(I)}$ and $Fe_{(II)}$ sites of kaolinites resulting from spin resonance arising from the three Kramer's doublets, whose energies are separated by crystal fields of rhombic symmetry.[17] $Fe_{(I)}$ and $Fe_{(II)}$ are two unequivalent crystal sites which Fe^{+3} can occupy in the octahedra in kaolinite.[17,18]

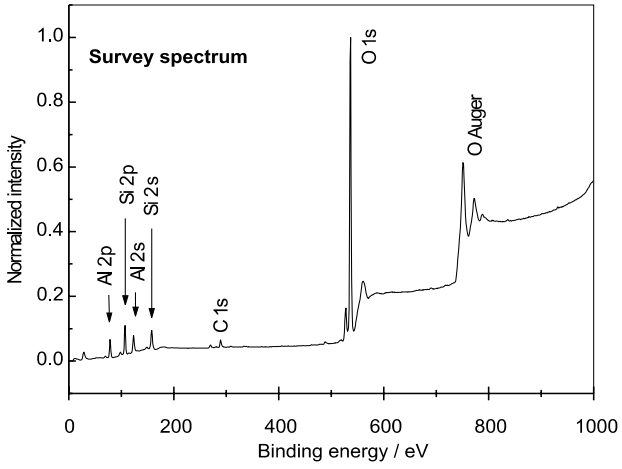

Figure 4. XPS wide scan spectrum of PP-0559 kaolinite

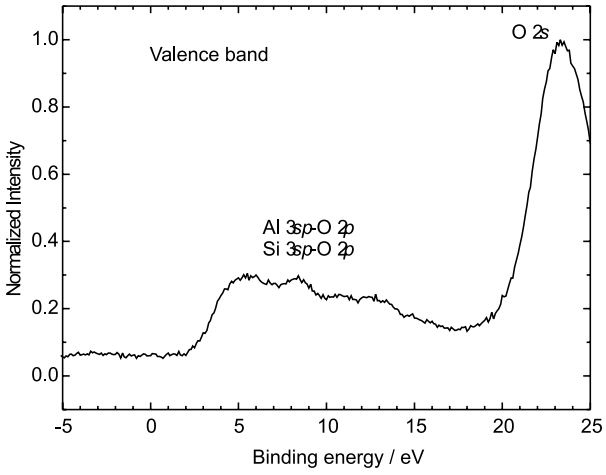

Figure 5. XPS valence band spectrum of PP-0559 kaolinite

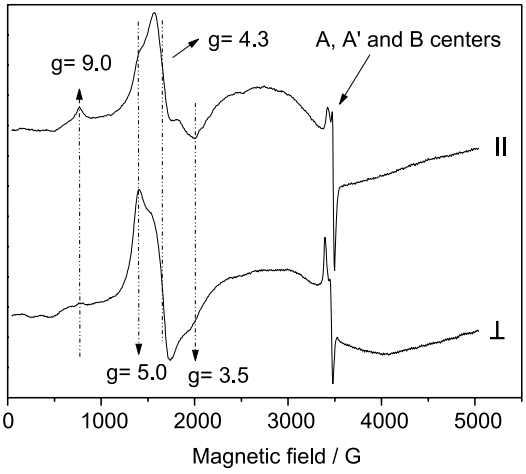

Figure 6. EPR spectra of PP-0559 kaolinite oriented parallel and perpendicular to the applied magnetic field, in the first derivative mode

The energy levels are sorted in ascending order from 1 to 6.[17] The resonance line with g = 9.0 results from the so called 12Y, 1 → 2 transition, between the energy levels 1 and 2, m_s = -5/2 to m_s = -3/2, in the y axis direction. The three lines with g-values of 5.0, 3.5 and 2.8 arise from the angular dependence of the spin transition inside the central doublet, m_s = -1/2 (3) to m_s = + ½ (4). Those are thus refereed as 34Z, 34X and 34Y transitions, in the z, x and y directions, respectively.

Some transitions are detected and others are not. There are two problems involved here: a) The allowed transitions, 1 → 2, 2 → 3, 3 → 4..., have different transition probabilities and therefore different intensities. b) Some transitions occur out of the energy range determined by the frequency or the field sweep used in the spectrometer for spectra recording. The g = 4.3 line is also a 34XYZ transition but isotropic in nature.

These two Fe^{3+} sites are localized in dilute domains and show different distortions.[18] The resonance near g = 9.0 and the isotropic signal centered at g ~ 4.3 are attributed to the $Fe_{(I)}$ center, that has a zero-field splitting terms D and E relation, E ≅ D/3, corresponding to rhombically distorted sites. The $Fe_{(II)}$ center, with resonances near g = 5.0, 3.5 and 2.8, has the relation E ≅ D/4. So, this kind of iron center is more symmetrical than the center with the E = D/3 relation. The kaolinite analyzed in this work has two kinds of Fe^{3+} centers.

In the parallel spectrum (Figure 6) the intensities of the lines with g-values of 2.8 (34Y), 3.5 (34X) and 9.0 (12Y) are higher than in the perpendicular spectrum. The isotropic line with g = 4.3 presents roughly similar intensity in both the parallel and perpendicular spectra as predicted. The intensity of the line with g = 5.0, a 34Z line, decreases from the perpendicular to the parallel spectrum. In consequence, considering a coordinated system with the z axis perpendicular to the kaolinite sheets, we conclude that the kaolinite sheets stayed, preferentially, parallel to the plane of the cavity of the EPR tissue cell.

Figure 7 shows the second derivative mode EPR spectra at a field range of 200 G of the same kaolinite sample. The signals details are better shown in the second derivative mode where even the signal/noise ratio decreases.

Evidence of preferential orientation of the A, A' and B centers is shown as follows. The A' center lines ($g_\perp$ = 2.0097) have their parallel absorption ($g_{||}$ = 2.0403) intensified in the parallel spectrum, indicating that the Si-O^- bonds of this center are localized parallel to the kaolinite sheet (Figure 1). On the perpendicular spectrum the absorption corresponding to the parallel spectrum of the A center ($g_{||}$ = 2.0526) is intensified, showing that Si-O^- bonds of this center are localized perpendicularly to the kaolinite sheet (Figure 1). In this orientation a sextet of lines belonging to the B paramagnetic center is also intensified. These centers exhibit a hyperfine structure (^{27}Al nucleus, I = 5/2), with the hyperfine coupling constant, A = 7 G. The observation of these lines suggest that, at least, one of the magnetization axes of the Al-O^- structure is localized perpendicularly to the kaolinite sheet (Figure 1).

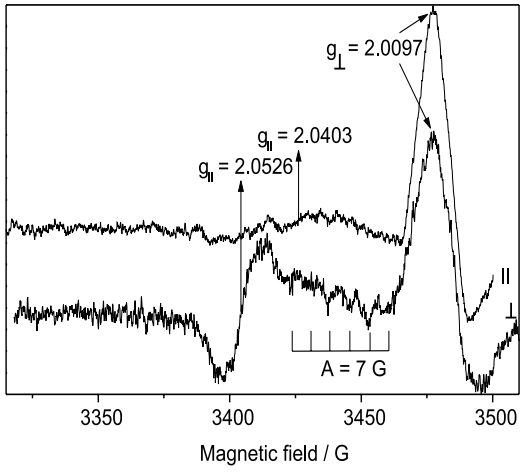

Figure 7. EPR spectra of PP-0559 kaolinite oriented parallel and perpendicular to the applied magnetic field, in the second derivative mode

Conclusions

This kaolinite from the Amazon basin is a very low defect clay mineral, as can be seen on the X ray diffractogram and the transmission electron micrographs. This kaolinite forms very defined monocrystalline platelets of up to 2 μm and can be readily oriented due to this anisotropy. The XPS results show that this natural mineral is of very high purity, while the valence band reveals an insulator with broad peak features due to Al, Si 3p and 3s and O 2p bonding molecular orbitals. Detailed EPR measurements with the platelets oriented parallel and perpendicular to the applied magnetic field revealed more strucutural details of the $F_{(I)}$ and $Fe_{(II)}$ sites absorption lines, as well as the orientation of the A, A' and B paramagnetic radiation induced defect centers.

Acknowledgments

The financial support of the following Brazilian agencies is gratefully acknowledged: PRONEX, FINEP, COPEL, CAPES and CNPq. Thanks are also due to the Centro de Microscopia Eletrônica from the UFPR.

References

1. Mangrich, A.S.; Lobo, M.A.; Tanck, C.B.; Wypych, F.; Toledo, E.B.S.; Guimarães, E.; *J. Braz. Chem. Soc*. **2000**, *11*, 164.
2. Novotny, E.H.; Blum, W.E.H.; Gerzabek, M.H.; Mangrich, A.S.; *Geoderma* **1999**, *92*, 87.
3. Russel, J.D.; Fraser, A.R. In *Clay Mineralogy*; Wilson, M.J., ed.; Chapman & Hall: London, 1994, p 11.
4. Muller, J.P.; Manceau, A.; Calas, G.; Allard, T.; Ildefonse, P.; Hazemann, J.L.; *Amer. J. Sci*. **1995**, *295*, 1115.
5. Ghazi, M.; Barrault, J.; *Bull. Soc. Chim. Belg*. **1992**, *101*, 755.
6. Schroeder, P.A.; Pruett, R.J.; *Amer. Miner*. **1996**, *81*, 26.
7. Gaite, J.M.; Ermakoff, P.; Allard, T.; Muller, J.P.; *Clays Clay Miner*. **1997**, *45*, 49.
8. Clozel, B.; Allard, T.; Muller, J.P.; *Clays Clay Miner*. **1994**, *42*, 657.
9. Allard, T.; Muller, J.P.; Dran, J.C.; Menager, M.T.; *Phys. Chem. Miner*. **1994**, *21*, 85.
10. Gardolinski, J.E.; Pereira Ramos, L.; Pinto de Souza, G.; Wypych, F.; *J. Colloid Interface Sci*. **2000**, *21*, 284.
11. Grim, R. F.; *Clay minerals*, McGraw-Hill: New York, 1953.
12. JCPDS - Joint Committee on Powder Diffraction Standards, File: 14-164; American Society For Testing and Materials, USA, ASTM, 1965.
13. Briggs, D.; Seah, M.P.; *Practical Surface Analysis by Auger and X ray Photoelectron Spectroscopy*, Wiley: Chichester, 1995, ch. 1.
14. Moulder, J.F.; Stickle, W.F.; Sobol, P.E.; Bomben, K.D.; *Handbook of X ray Photoelectron Spectroscopy*, Physical Electronics INC. ed.: Eden Prairie; USA, 1995, ch. 1.
15. Kim, Y.; Cygan, R.T.; Kirkpatrick, R.J.; *Geochim. et Cosmochim. Acta* **1996**, 60, 1041.
16. Barr, T.L.; Seal, S.; He, H.; Klinowski, J.; *Vacuum* **1995**, 46, 1391.
17. Balan, E.; Allard, T.; Boizot, B.; Morin, G.; Muller, J.P.; *Clays and Clay Miner.*, **2000**, *48*, 439.
18. Balan, E.; Allard, T.; Boizot, B.; Morin, G.; Muller, J.P.; *Clays and Clay Miner.*, **1999**, 47, 605.
19. The Virtual Museum of Minerals and Molecules™, (2000), 3D representations of minerals and molecules: http://www.soils.wisc.edu/virtual_museum, *accessed in march* 2001.

Received: April 9, 2001
Published on the web: March 26, 2002